portin-β for FG nucleoporins by altering the relative positions of HEAT repeats 5 and 6 (*7*, *8*); this change also facilitates cargo release.

Crystallography has defined the interaction interfaces between importin-β and many of its binding partners. FG nucleoporins bind on the outer, convex surface of importin-β to a primary site between HEAT repeats 5 and 6 and to several secondary sites, including one near the carboxyl terminus (*7*, *8*, *15*). However, the remainder of importin-β's binding partners interact primarily with the inner, concave face. RanGTP binds to HEAT repeats 1 to 8 at the amino terminus of importin-β (*4*), whereas the mainly helical IBB domain binds over an extensive area of the concave surface that encompasses HEAT repeats 7 to 19 (*3*). The interface between IBB and importin-β exhibits an extended network of interactions involving more than 40 electrostatic, hydrophobic, and van der Waals contacts. Tryptophan residues (especially tryptophan-864) in importin-β help to stabilize the helical conformation of the IBB domain and so ensure specific, high-affinity binding (*16*). By contrast, the NLS of PTHrP (parathyroid hormone–related protein) binds at the importin-β amino terminus (HEAT repeats 2 to 6) and overlaps with the RanGTP binding site (*9*). This NLS adopts primarily a β-sheet conformation, and its interaction is reminiscent of the way classic NLSs bind to importin-α (*6*). Although the binding sites for the PTHrP-NLS and IBB domain on importin-β partly overlap, the molecular architecture of their sites is different and both can bind to importin-β simultaneously (*9*).

SREBP-2 lacks a classic NLS and, as Lee *et al*. (*10*) describe, binds to importin-β via its dimeric helix-loop-helix zipper (HLHZ) domain. As the investigators show, the crystal structure of the importin-β:SREBP-2 complex reveals a remarkable new twist in the way that importin-β recognizes its cargo. In this complex, the dimeric HLHZ domain is gripped primarily by the long α helices of HEAT repeats 7 and 17 that move like chopsticks to pick up the cargo. In contrast to the IBB domain α helix, the α helices of the HLHZ domain are perpendicular to the central axis of the importin-β superhelix. To accommodate this interaction, importin-β moves the long helices of HEAT repeats 7 and 17 and adopts a more twisted and open conformation. The conformational change introduced in this way is dramatic, with the amino-terminal region moving by 20 Å (a rotation of 22°). In contrast to the PTHrP-NLS and the IBB domain, the interaction between importin-β and the HLHZ domain of SREBP-2 is mediated primarily by hydrophobic interactions; charge complementation is of less importance. Lee *et al.* also note the presence of a possible structural repeat in the sequence of importin-β that offers a convenient way for importin-β to bind to dimeric cargo proteins and perhaps also to FG nucleoporins (*15*).

Overall, the remarkable conformational variability of importin-β:cargo complexes implies that unbound free importin-β is flexible and so can adapt its shape to recognize a variety of different partners. Such flexibility is consistent with the greater susceptibility of free versus bound importin-β to proteolysis (*3*). Although high-resolution structures of different binding states have not yet been obtained, several homologs of importin-β probably also provide an analogous flexible scaffold that facilitates versatility in substrate recognition (*14*). By contrast, although importin-α interacts with a range of substrates, these interactions do not appear to involve major conformational changes, even when they accelerate the rate of cargo release (*17*).

That importin-β must bind to a remarkable range of different proteins to carry out both its nuclear trafficking and nuclear assembly tasks exerts extraordinary demands on molecular recognition capabilities. Such demands are made even more pressing by the necessity for importin-β to bind to and release many of its partners in a spatially and temporally defined sequence. Molecular recognition usually involves matching of complementary interfaces between interacting proteins, and it is not uncommon for relatively small structural alterations to be present at the interface associated with binding, or for domains of molecules to rotate around a hinge. However, the conformational changes observed when importin-β binds to its partners, particularly when it binds to SREBP-2, involve an unusually large distortion. Although stacking of 19 tandem HEAT repeats generates an extensive interaction surface that enables importin-β to bind to a wide range of different molecules, importin-β supplements this ability with a remarkable degree of conformational flexibility. In this way, it is able to greatly increase its versatility in recognizing and releasing its different binding partners. As more crystal structures of importin-β bound to different cargo proteins become available, it will be fascinating to see how the interplay of surface structure and conformational dynamics is exploited to accomplish a variety of different tasks.

References

1. K. Weis, *Cell* **112**, 441 (2003).
2. Y. M. Chook, G. Blobel, *Nature* **399**, 230 (1999).
3. G. Cingolani *et al.*, *Nature* **399**, 221 (1999).
4. I. R. Vetter *et al.*, *Cell* **97**, 635 (1999).
5. Y. M. Chook, G. Blobel, *Curr. Opin. Struct. Biol.* **11**, 703 (2001).
6. E. Conti, E. Izaurralde, *Curr. Opin. Cell Biol.* **13**, 310 (2001).
7. R. Bayliss *et al.*, *Cell* **102**, 99 (2000).
8. R. Bayliss *et al.*, *J. Biol. Chem.* **277**, 50597 (2002).
9. G. Cingolani *et al.*, *Mol. Cell* **10**, 1345 (2003).
10. S. J. Lee *et al.*, *Science* **302**, 1571 (2003).
11. B. Fahrenkrog, U. Aebi, *Nature Rev. Mol. Cell Biol.* **4**, 757 (2003).
12. C. Zhang *et al.*, *Curr. Biol.* **12**, 498 (2002).
13. A. Harel *et al.*, *Mol. Biol. Cell* **14**, 4387 (2003).
14. N. Fukuhara *et al.*, *J. Biol. Chem.* M309112200 (2003).
15. J. Bednenko *et al.*, *J. Cell Biol.* **162**, 391 (2003).
16. C. Koerner *et al.*, *J. Biol. Chem.* **278**, 16216 (2003).
17. Y. Matsuura *et al.*, *EMBO J.* **22**, 5358 (2003).

OCEAN SCIENCE

The Many Shades of Ocean Blue

Hervé Claustre and Stéphane Maritorena

In satellite data over the South Pacific gyre, Earth's largest oceanic desert (see the figure), Dandonneau *et al*. [page 1548 of this issue (*1*)] have detected areas that are greener than the surrounding deep blue waters. They suggest that these "hotspots" are not vegetal oases, but rather result from residues and by-products of marine life accumulated by physical processes. This detrital material would be incorrectly interpreted as phytoplankton biomass from satellite ocean color data. The study provides further evidence that the current paradigm—the greener the open ocean waters, the higher their phytoplankton content—has its limitations.

H. Claustre is at the Observatoire Océanologique de Villefranche, Laboratoire d'Océanographie de Villefranche, CNRS-INSU, 06238 Villefranche-sur-mer, France. E-mail: claustre@obs-vlfr.fr S. Maritorena is at the Institute for Computational Earth System Science, University of California, Santa Barbara, CA 93106, USA. E-mail: stephane@icess.ucsb.edu

For nearly 25 years, ocean color has been used as a proxy for algal biomass. Empirical algorithms (*2*) for mapping the global phytoplankton distribution from space rely on mean statistical relationships between the chlorophyll a concentration [Chla] (a proxy for phytoplankton biomass) and the blue-to-green (B/G) reflectance ratio (an optical index for water color). The resulting [Chla] maps are used to estimate the contribution of phytoplankton to global CO_2 fixation (*3*) and investigate long-term changes in vegetal biomass (*4*).

However, there is increasing evidence that the simple empirical relationship between [Chla] and B/G ratio does not always hold. Which optically active components cause these deviations, and where do they occur? Answers to these questions should shed light on regional ecosystem structure and functioning.

Phytoplankton itself is one of the first candidates to be examined. Marine phyto-

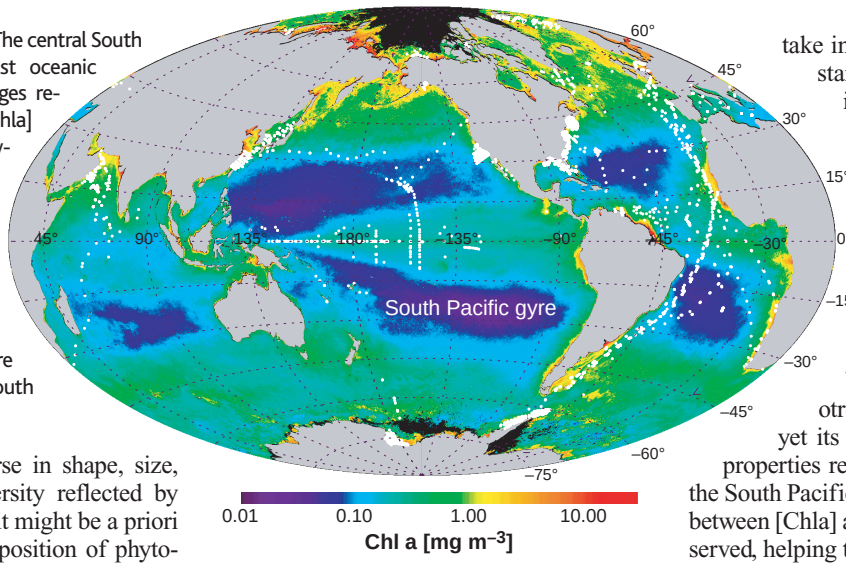

Colors of an oceanic desert. The central South Pacific gyre is Earth's largest oceanic desert. SeaWiFS satellite images reveal its consistently low [Chla] (deep blue and purple). However, some nuances in the blue color of these waters can be detected (*1*). Only 20% of available measurements (white symbols) for ocean color algorithms development have been collected in the Southern Hemisphere (and less than 2% in the South Pacific between 0° and 60°S).

CREDIT: DATA COURTESY OF THE NASA SEAWIFS AND SIMBIOS PROJECTS

plankton are highly diverse in shape, size, and pigmentation, a diversity reflected by their varying color. Thus, it might be a priori possible to track the composition of phytoplankton communities from space. For example, *Emiliania huxleyi* is covered with calcium carbonate plates that, when released in the water, give it a milky turquoise color, easily captured by satellite (*5*). *Trichodesmium* sp.'s gas vesicles and specific pigmentation may also allow its remote detection (*6*). However, apart from *E. huxleyi* and *Trichodesmium* sp., discriminating phytoplankton types from space is difficult, because detected nuances could easily be confounded with noise.

Besides phytoplankton, colored dissolved organic matter (CDOM) and submicrometer detritus particles also affect the optical properties of oceanic waters. CDOM is responsible for a large (sometimes dominant) fraction of the visible blue light absorbed by the water (*7*). Assessments of [Chla] from empirical ocean color algorithms can be skewed by the presence of such dissolved material.

Absorption by submicrometer particles is generally small compared to that of phytoplankton or CDOM. However, these particles are a major source of backscattered light in the open ocean. Underestimates of [Chla] at high latitudes have been attributed to low backscattering, possibly because of low concentrations of submicrometer particles, either detritus or living (bacteria, viruses) (*8*). Conversely, a phytoplankton bloom could rapidly be transformed into detrital material by viruses (*9*), leading to overestimates of [Chla].

Recent studies have also suggested that fine desert dust trapped in the upper layer of the ocean might depress the B/G ratio, causing overestimates of [Chla] (*10*). Dust deposition is associated with the dissolution of iron, an important phytoplankton fertilizer. Future studies aiming to assess the impact of desert dust deposition on marine biogeochemical cycles must discriminate between the enhanced backscattering due to the dust and the increased phytoplankton biomass due to fertilization (*11*).

The story becomes even more complex with the presence of bubbles, which make the water appear greener (*12*). Hence, the rougher the sea state and the higher its bubble content, the more standard algorithms would overestimate [Chla].

Present empirical models are not well suited to capture the impact of these optically active components. Furthermore, ocean color algorithms have been established from data collected mostly in the Northern Hemisphere, with few data points from very oligotrophic areas. They might therefore not represent the Southern Hemisphere well, particularly the central part of the gyres, which also experience lower dust deposition. Semianalytical algorithms must be developed that explicitly take into account the various substances that affect ocean color in both hemispheres (*7*, *13*). Further in situ investigations in the Southern Hemisphere are also needed, especially in remote areas such as the South Pacific gyre investigated by Dandonneau *et al.* (*1*) (see the figure). This vast oceanic biome is the most oligotrophic water body on Earth, yet its optical and biogeochemical properties remain largely unexplored. In the South Pacific gyre, new types of nuances between [Chla] and ocean color might be observed, helping to explain the various shades of ocean blue.

References

1. Y. Dandonneau *et al.*, *Science* **302**, 1548 (2003).
2. J. E. O'Reilly *et al.*, *J. Geophys. Res.* **103,** 24937 (1998).
3. D. Antoine *et al.*, *Global Biogeochem. Cycles* **10**, 57 (1996).
4. M. C. Gregg, M. A. Conkright, *Geophys. Res. Lett.* **29** (15), 10.1029/2002GL014689 (2002).
5. P. Holligan *et al.*, *Nature* **304**, 339 (1983).
6. A. Subramaniam *et al.*, *Deep Sea Res. II* **49**, 107 (2002).
7. D. A. Siegel *et al.*, *J. Geophys. Res.* **107**, 3228 (2002).
8. H. M. Dierssen, R. C. Smith, *J. Geophys. Res.* **105**, 26301 (2000).
9. W. M. Balch *et al.*, Abstract 663, *ASLO/TOS Ocean Research Conference*, Honolulu, Hawaii, 15 to 20 February 2004.
10. H. Claustre *et al.*, *Geophys. Res. Lett.* **29** (10), 10.1029/2001GL014056 (2002).
11. J. K. B. Bishop *et al.*, *Science* **298**, 817 (2002).
12. D. Stramski, J. Tegowski, *J. Geophys. Res.* **106**, 31345 (2001).
13. H. Loisel, D. Stramski, *Appl. Opt.* **39**, 3001 (2000).

IMMUNOLOGY

The Paracaspase Connection

Li Yu and Michael J. Lenardo

Successful immune responses depend on the regulation of many genes to guide the biological effects of T and B lymphocytes. To accomplish this, various incoming signals must be integrated and then distributed to a diverse set of gene expression outputs. The transcription factor NF-κB serves as a key signal integrator in this process in ways that no one could have imagined when it was first identified as a DNA binding factor (*1*, *2*). On page 1581 of this issue and in the most recent issue of *Immunity*, the laboratories of Dixit and Mak, respectively, reveal that a mouse protein called MALT1/Paracaspase (MPC) is a crucial regulator of NF-κB activity in B and T cells (*3, 4*).

Numerous cytokines, chemical mediators, and cell surface receptors, including the antigen receptors of B and T lymphocytes, activate NF-κB. Nuclear NF-κB can bind to and regulate the DNA control elements of a wide variety of immune response genes [reviewed in (*5*)]. The centerpiece of the NF-κB pathway is the IκB kinase (IKK) complex (*6*). IKK is formed from three subunits (IKKα, IKKβ, and IKKγ/NEMO) that transduce diverse upstream signals into the phosphorylation and degradation of IκB, the inhibitory binding partner that restrains NF-κB in the cytoplasm. When IκB is degraded, NF-κB is

The authors are in the Laboratory of Immunology, National Institute of Allergy and Infectious Diseases, Bethesda, MD 20892, USA. E-mail: mlenardo@nih.gov